MOLECULAR AND CELLULAR BIOLOGY, Jan. 2008, p. 642–655 Vol. 28, No. 2
0270-7306/08/$08.00+0 doi:10.1128/MCB.01024-07

c-Src-Mediated Epithelial Cell Migration and Invasion Regulated by PDZ Binding Site▽†

Martin Baumgartner,* Gerald Radziwill,‡ Mihaela Lorger,‡§ Andreas Weiss,¶ and Karin Moelling

Institute of Medical Virology, University of Zürich, Gloriastrasse 30, 8006 Zürich, Switzerland

Received 11 June 2007/Returned for modification 28 July 2007/Accepted 1 November 2007

c-Src tyrosine kinase controls proliferation, cell adhesion, and cell migration and is highly regulated. A novel regulatory mechanism to control c-Src function that has recently been identified involves the C-terminal amino acid sequence Gly-Glu-Asn-Leu (GENL) of c-Src as ligand for PDZ domains. Herein, we determined the biological relevance of this c-Src regulation in human breast epithelial cells. The intact GENL sequence maintained c-Src in an inactive state in starved cells and restricted c-Src functions that might lead to metastatic transformation under normal growth conditions. c-Src with a C-terminal Leu/Ala mutation in GENL (Src-A) promoted the activation and translocation of cortactin and focal adhesion kinase and increased the motility and persistence of cell migration on the basement membrane. Src-A promoted increased extracellular proteolytic activity, and in acinar cultures, it led to the escape of cells through the basement membrane into the surrounding matrix. We ascribe the regulatory function of C-terminal Leu to the role of GENL in modulating c-Src activity downstream of cell matrix adhesion. We propose that the C terminus of c-Src via its GENL sequence presents a mechanism that restricts c-Src in epithelia and prevents progression toward an invasive phenotype.

c-Src is a nonreceptor tyrosine kinase that is essential for the regulation of a wide range of cellular functions, including cell proliferation and cell migration (18, 35). Src family kinases regulate cell migration in normal and oncogenically transformed cells by modifying cell-cell and cell-matrix adhesions (3, 4, 13, 21, 27) and by promoting the expression of matrix-modifying proteases (39, 54). The regulation of c-Src and its analogs is complex and involves the reversible phosphorylation of Y416 and Y527, as well as protein-protein interactions through its Src homology 2 (SH2) and SH3 domains (8). It is speculated that an additional mechanism may involve the displacement of an N-terminal myristate from and the subsequent binding of the C terminus of c-Src to a hydrophobic lobe in the catalytic domain (15).

c-Src integrates its activity into intracellular signaling networks in normal and transformed cells through substrates including focal adhesion kinase (FAK) and cortactin. FAK is a cytoplasmic tyrosine kinase that is a key element in integrin-stimulated signaling networks (47). c-Src binds FAK directly and promotes the phosphorylation of C-terminal Y861 and Y925 in FAK and the activation of multiple intracellular signaling pathways. FAK is required for cell migration (26), and FAK and Src synergize in cell migration and invasion (12, 24). Cortactin is a target of multiple kinases, including Src at Y421, and acts thereby as a regulated scaffold to promote actin polymerization and F-actin branching (14). Cortactin regulates cell migration by increasing actin polymerization (31) and by enhancing lamellipodial persistence (11). Cortactin localizes to sites of active invadopodia (9), where it functionally cooperates with activated c-Src and membrane type 1-matrix metalloproteinase (MT1-MMP) in matrix degradation (2).

Proper regulation of Src kinases is important, and C-terminal deletion from the viral oncogene v-Src in the Rous sarcoma virus leads to deregulated Src activity and oncogenic transformation (18, 35). Deregulation of c-Src is believed to play an important role in human tumorigenesis by promoting proliferation, survival, and migration (27). c-Src protein levels are increased in a number of human breast tumor cell lines (7), and the expression of kinase-inactive Src or small interfering RNA strategies reverted the properties of human MCF7 breast tumor cells, such as increased proliferation and motility (21). In human breast epithelial acinar structures, c-Src functions downstream of activated growth factor receptors and is required for the disruption of acinar morphology (52).

c-Src, Yes, and Fyn harbor at their very C termini a class III PDZ domain binding sequence, Gly-Glu-Asn-Leu (GENL), and this sequence is involved in the regulation of Src kinase function in cells (44). GENL mediates its inhibitory function through a novel C-terminal Leu-dependent interaction with the PDZ protein AF6. PDZ proteins are a large family (785 PDZ domains in 436 proteins) with a high degree of functional diversity, and PDZ proteins other than AF6 are likely to functionally interact with c-Src in cells (44). PDZ proteins coordinate supermolecular protein complexes at epithelial cell-cell contacts (42) and in neuronal synapses (29). PDZ domains are 80- to 90-residue-long protein-protein interaction domains that recognize short peptide motifs, PDZ domain ligands such as GENL, ending with a hydrophobic residue for which three different classes are described (42).

* Corresponding author. Mailing address: Institute of Medical Virology, University of Zürich, Gloriastrasse 30, CH-8006 Zürich, Switzerland. Phone: 41 44 634 44 20. Fax: 41 44 634 49 67. E-mail: Martin.Baumgartner@immv.uzh.ch.

§ Present address: Scripps Research Institute, 10550 North Torrey Pines Road, La Jolla, CA 92037.

¶ Present address: Unit of Experimental Immunotherapy, Department of Dermatology, University Hospital Zürich, Zürich, Switzerland.

‡ G.R. and M.L. contributed equally to this work.

† Supplemental material for this article may be found at http://mcb.asm.org/.

▽ Published ahead of print on 26 November 2007.

c-Src regulation by PDZ proteins might be of particular importance in epithelial cells to maintain cell polarity and multicellular integrity. Therefore, we investigated whether c-Src with a defective PDZ binding sequence, GENA (Src-A), interfered with epithelial cell function with two- and three-dimensional cell cultures. We used the nontransformed human breast epithelial cell line MCF-10A for studying the GENL-dependent regulation of c-Src functions during cell adhesion, in cell migration, and during the formation of acinar cultures. MCF-10A acinar cultures have been used to investigate the development of a single cell to a multicellular, polarized structure (16, 40, 43) and the pathways that are targeted by oncogenes (40, 52). We describe the importance of the intact C-terminal PDZ ligand sequence GENL in c-Src for preventing aberrant c-Src functions in epithelial cells that may lead to invasive cell behavior.

MATERIALS AND METHODS

Cells. The MCF-10A cells were obtained from the American Type Culture Collection and grown in complete growth medium (Dulbecco's modified Eagle's medium plus Ham F12 [DME-F12] with 2 mM L-glutamine supplemented with 20 ng/ml epidermal growth factor [EGF; Sigma], 100 ng/ml cholera toxin [Sigma], 10 ng/ml insulin [Sigma], 500 ng/ml hydrocortisone [Sigma], and 5% horse serum). Starvation medium is DME-F12 without supplements. Tetracycline (Tet)-inducible Tet-off cell lines were generated by transducing MCF-10A cells with the pRTP retrovirus vector (22) encoding either the Src-L or the Src-A mutation (44). Chicken c-Src amino acid numbering is used throughout this article. For Src-L and Src-A expression, 100 ng/ml Tet was removed 24 h before the experiment. EGF stimulations were performed using 20 ng/ml EGF. HEK293 cells were grown and transfected as described previously (44).

Cell lysis, Wb, and antibodies. Cells were lysed in modified radioimmunoprecipitation assay buffer containing 150 mM NaCl, 50 mM Tris (pH 7.4), 1 mM EDTA (pH 8.0), 1.0% NP-40, 0.25% Na-deoxycholate, 2 mM Na-vanadate, 25 mM NaF, and a protease inhibitor cocktail (Roche). Western blotting (Wb) was carried out using standard procedures. The antibodies used were mouse monoclonal anti-Src clone GD11 and anti-phospho-Tyr4G10 (Upstate); rabbit polyclonal anti-Src2, anti-focal adhesion kinase c-20, anti-cortactin H-191, and anti-extracellular signal-regulated kinase 2 (anti-ERK2) c-14 (Santa Cruz Biotechnology); anti-phospho-Y861 focal adhesion kinase and anti-phospho-Y421 cortactin (Biosource); anti-phospho-Y416 Src family, anti-phospho-Y527 Src, and anti-phospho-p44/42 mitogen-activated protein kinase (MAPK; Cell Signaling Technology); antigiantin (Covance); anti-MT1-MMP (catalog no. AB8345); and anti-laminin-5 γ2 chain (catalog no. MAB19562) (Chemicon). MPP2 is a custom-made (Eurogentec) rabbit polyclonal antibody raised against a peptide in the C terminus of human MPP2. Integrated pixel densities from Wbs were quantified using NHI image software.

Cell fractionation. Cells were scraped into sonication buffer (50 mM HEPES [pH 7.4], 135 mM NaCl, 3 mM KCl, 3 mM EDTA, 2 mM Na-vanadate, 25 mM NaF, and a protease inhibitor mini cocktail [Roche]) and sonicated by three 15-s pulses (at 18 W). Nuclei and intact cells were pelleted by centrifugation at 850 × *g* for 5 min. Supernatant containing 400 μg of protein (postnuclear supernatant) was recovered and centrifuged at 100,000 × *g* for 20 min at 4°C to obtain a soluble fraction (S100). For Triton extraction, S100 membrane pellets were incubated for 1 h at room temperature in the sonication buffer containing 1.0% Triton X-100 (TX-100). Extracted membranes were centrifuged at 100,000 × *g*, as described above, to obtain TX-100-soluble (P100 TX-100 sol.) and TX-100-insoluble (P100 TX-100 insol.) fractions. All fractions were solubilized in Laemmli sample buffer. One-twentieth of S100, 1/4 of P100 TX-100 sol., and 1/4 of P100 TX-100 insol. solutions were used for sodium dodecyl sulfate-polyacrylamide gel electrophoresis (SDS-PAGE) and Wb.

Csk assay. Hemagglutinin (HA)-tagged Src proteins were produced by coupled in vitro transcription/translation (using a reticulocyte lysate kit; Promega). HA-tagged proteins were immunoprecipitated from reticulocyte lysates and subjected to kinase reaction mixtures with the following components: 50 mM Tris (pH 7.5), 1 mM EGTA, 0.1% 2-mercaptoethanol, 0.1 mM Na_3VO_4, 10 mM $MnCl_2$, 15 mM $MgCl_2$, 100 μM ATP, 4 mM morpholinepropanesulfonic acid, 5 mM β-glycerol phosphate, 0.2 mM dithiothreitol with or without 100 ng C-terminal Src kinase (Csk; Upstate) per reaction. Reactions were carried out at 30°C for 20 min.

Immunofluorescence microscopy. Cells were fixed in 3.6% formaldehyde at room temperature for 15 min or in 100% methanol at −20°C for 2 min, permeabilized with 0.5% TX-100 for 5 min, and blocked with 10% fetal bovine serum in phosphate-buffered saline. Primary antibodies were used at 1/200 dilution in 5% fetal bovine serum in phosphate-buffered saline. Secondary anti-mouse or anti-rabbit antibodies (Jackson ImmunoResearch) coupled to fluorescein isothiocyanate or tetramethylrhodamine isothiocyanate were used for detection. Confocal image stacks were acquired with an inverted Leica SP5 microscope through a Leica 63× oil objective, recorded with a Leica camera, and analyzed with Imaris version 5.3 software. Fluorescence intensities of polarized migrating cells (broad, flat lamella at the front and at trailing edges at the rear) were quantified using NIH image software.

Cell migration assays. For wound healing assays, confluent cells were starved in starvation medium for 18 h. Wounds were created by scratches with pipette tips. Cells were incubated with or without 20 ng/ml EGF in a temperature-controlled and CO_2-controlled climate chamber mounted onto a Leica inverted microscope. Time-lapse images were captured every 10 min for 15 h using a Hamamatsu ORCA ER C4742-95 camera through a 10× Leica N Plan objective and operated by Openlab software. For single-cell migration, subconfluent cells were detached by trypsinization, recovered in trypsin inhibitor solution (Sigma), and resuspended and kept in suspension in the starvation medium for 1 h at 37°C. MCF-10A cell basement membrane (BM) was prepared as described previously (38). Briefly, MCF-10A cells were grown to confluence on the desired support and treated with 20 mM ammonium hydroxide to destroy the cells while preserving the BM. Cells were seeded onto the BM with or without 20 ng/ml EGF and incubated for 2 h at 37°C before being processed for immunofluorescence (IF) analysis. For single-cell migration analysis by live cell imaging, time-lapse images were captured every 4 min for 2 h as described above. To quantify cell movements, the localization of individual cells within an area of 600 by 600 digital pixels at *n* time points was recorded with Openlab as *x*/*y* values. A 2-h trajectory of the migrating cells was plotted with Excel based on 30 *x*/*y* values for each cell. Total distance (*d*) was determined as $d = \Sigma_{n=1-29}[(x_n - x_{n+1})^2 + (y_n - y_{n+1})]^{1/2}$. Velocity was quantified as *d*/*t* and expressed as μm/min (pixel size was 0.64 μm). Directionality was determined by dividing the direct distance (from the start to the end point) of each cell trajectory by the corresponding *d* value.

Golgi body reorientation measurements. The positions of the Golgi apparatus in migrating cells were determined according to the method described by Nobes and Hall (41).

Acinar culture growth in three-dimensional basement membrane cultures. Lab-TekII chamber slides were coated with 40 μl of Matrigel (BD Biosciences) per well. Cells (10^4) in 400 μl of complete medium containing 2% Matrigel were seeded per well on top of the solidified Matrigel. Medium was replaced with complete medium containing 2% Matrigel every 4 days.

Gelatin zymography. Cell extracts in Laemmli buffer without β-mercaptoethanol and without boiling were separated by SDS-PAGE in gels containing 1 mg/ml gelatin. Gels were incubated in 2.5% TX-100 for 30 min, and an in-gel protease cleavage reaction was performed thereafter in a buffer containing 50 mM Tris (pH 8.0), 200 mM NaCl, 5 mM $CaCl_2$, 0.02% Brij35 at 37°C overnight. Gelatin cleavage was revealed by Coomassie staining.

Statistics. A two-tailed Student *t* test was used for comparison between groups.

RESULTS

Negative regulation of c-Src by PDZ ligand sequence. We replaced the C-terminal leucine of c-Src with alanine, which impairs the interaction of c-Src with PDZ domains (44). c-Src proteins harboring this single-point mutation or wild-type c-Src proteins were expressed under a Tet-off promoter in MCF-10A cells, which are further referred to as the Src-A (alanine) and the Src-L (leucine) cells, respectively (Fig. 1A). The expression levels of endogenous c-Src, Src-L, and Src-A in MCF-10A cells in the presence and absence of Tet are shown in Fig. 1B.

To estimate the activation status of endogenous c-Src and the overexpressed Src-L and Src-A cells under normal growth conditions, we probed cell extracts with antiphosphotyrosine (Fig. 1B) or with activation-specific anti-phospho-Y416 (pY416) Src antibodies by Wb (Fig. 1C). Src-A cells grown in complete medium displayed similar levels of protein tyrosine

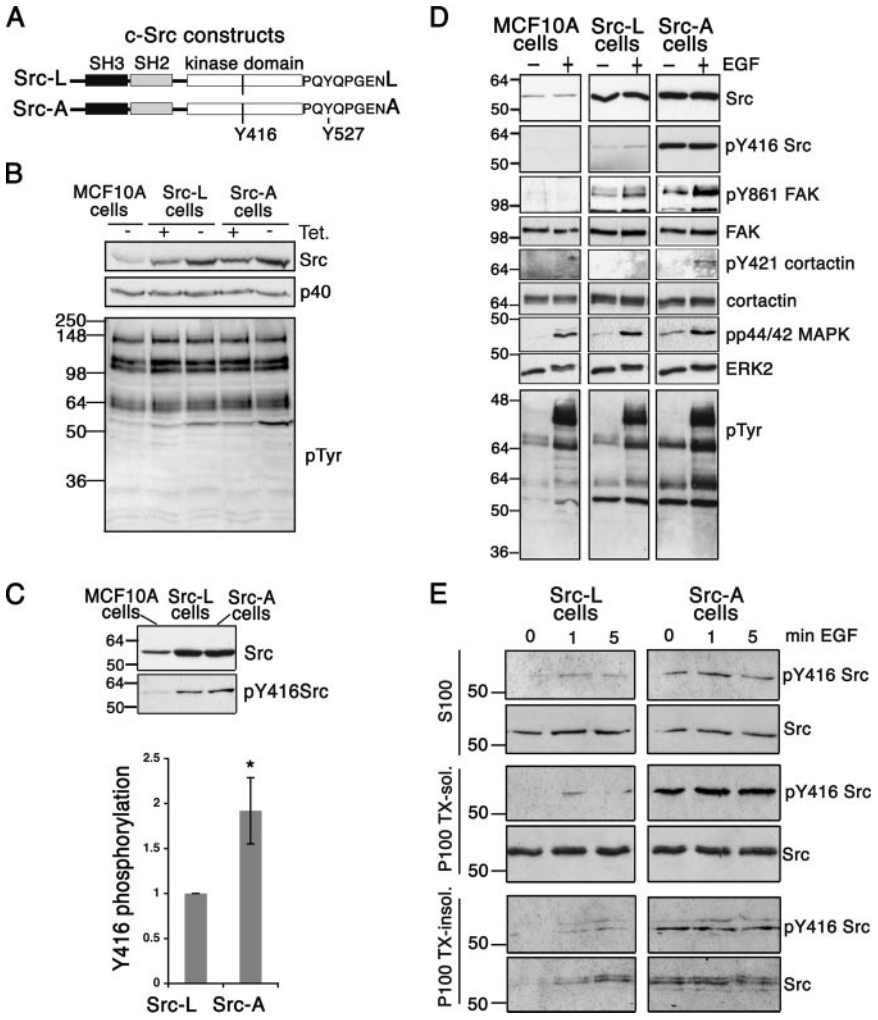

FIG. 1. C-terminal Leu/Ala substitution in PDZ ligand sequence GENL increases Src activity in cells. (A) Domain structure of Src-L and the Src-A mutant with the C-terminal Leu/Ala substitution. (B) Wb of total cell lysates of the Src-L and Src-A cells grown in complete medium with or without Tet, using anti-Src2 and anti-pTyr antibodies. P40 is a nonspecific band appearing in MCF-10A cell lysates probed with anti-Src2 antibody and serves as a loading control. (C) Wb of total cell lysates of the MCF-10A, Src-L, and Src-A cells grown in complete medium using anti-Src and anti-pY416 Src antibodies. The bar diagram shows average pY416 Src values from three independent experiments (error bars are standard errors of the means, $P = 0.034$). (D) Src-L and Src-A cells were serum starved and then stimulated with EGF for 5 min. Wbs of total cell lysates are shown, using the antibodies indicated. (E) Wbs of cellular fractionation are shown of Src-L or Src-A cells stimulated for 1 or 5 min with EGF, using anti-Src2 and anti-pY416 Src antibodies. Fractions included in Wb are high-speed supernatant, cytosolic fraction (S100), P100 TX-100 sol., and P100 TX-100 insol.

phosphorylation compared to that of control or Src-L cells (Fig. 1B), whereas the level of Y416 phosphorylation of the Src-A cells compared to that of the Src-L cells was moderately increased (Fig. 1C). In starved cells, Src-A activity was markedly increased compared to that of Src-L, likely accounting for the increased total tyrosine phosphorylation observed (Fig. 1D). EGF stimulation led to tyrosine phosphorylation of multiple proteins and increased the phosphorylation of Y861 in FAK, a Src-specific phosphorylation site (39). EGF stimulation resulted in the phosphorylation of Y421 of cortactin in Src-A cells but not in Src-L or in MCF-10A cells (Fig. 1D).

We next probed the cytosolic fraction (S100), the TX-100-soluble membrane fraction (P100 TX-100 sol.), and the TX-100-insoluble cytoskeleton fraction (P100 TX-100 insol.) for Src and Src Y416 phosphorylation activity (Fig. 1E). The Src-A Y416 phosphorylation in starved cells was increased compared to that in Src-L cells in all three subcellular fractions. After EGF stimulation, the Y416 phosphorylation of Src-L increased within 1 min, whereas the Y416 phosphorylation in Src-A did not change markedly. The amounts of Src-L and pY416 Src-L in the TX-100 insol. cytoskeleton fraction increased after EGF stimulation. Src-A was detectable in the TX-100 insol. cytoskeleton fraction, even in the absence of EGF stimulation. These data indicate a regulatory function of C-terminal Leu in starved cells by restricting activation of c-Src and by decreasing its association with membrane/cytoskeleton structures. Importantly, the phosphorylation of Y421 cortactin by Src-A after EGF stimulation also indicates that GENL restricts substrate recognition and phosphorylation by a mechanism that is independent of kinase activity.

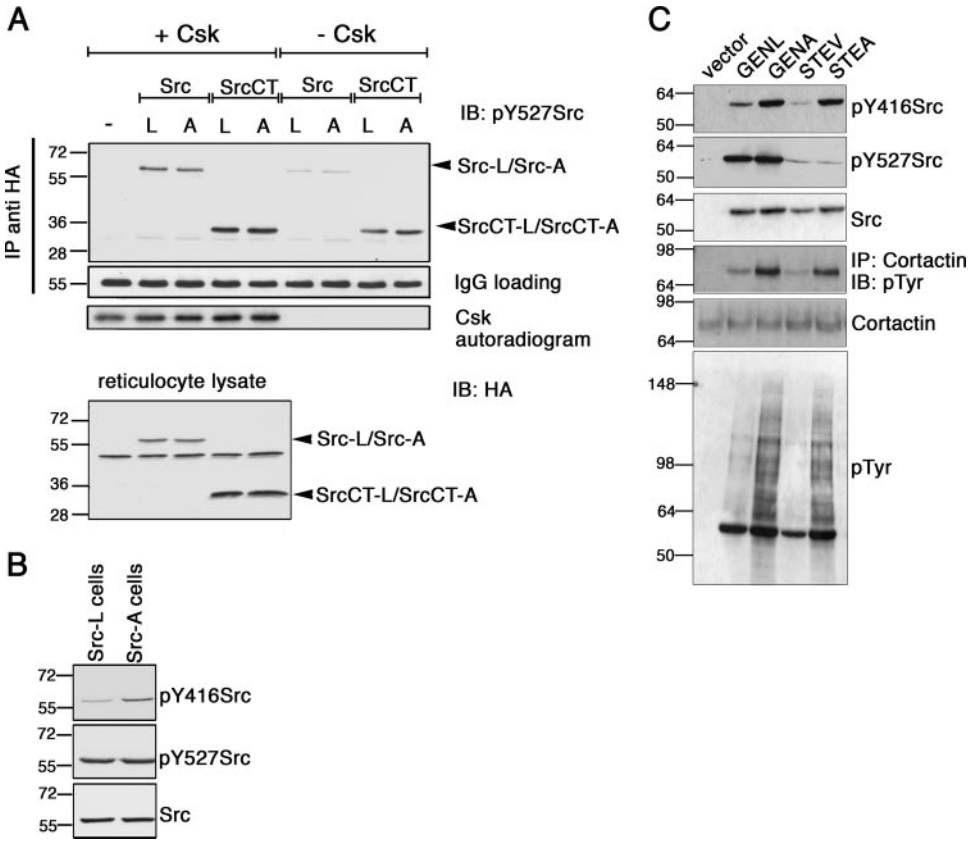

FIG. 2. Deregulated Src-A activity is independent of Csk and can be rescued by an alternative PDZ ligand. (A) HA-tagged full-length Src-L and Src-A or truncated (the kinase domain including the C terminus) SrcCT-L and SrcCT-A were expressed in reticulocyte lysates. Anti-HA immunoprecipitates were subjected to a kinase reaction with or without Csk. Tyr527 Src phosphorylation was detected by Wb. Expression controls for the individual proteins are shown below. (B) Wbs of the total cell lysates of Src-L and Src-A cells grown in complete medium using anti-pY416 Src, anti-pY527 Src, and anti-Src antibodies. (C) Src-L (GENL), Src-A (GENA), Src-STEV (STEV), and Src-STEA (STEA) were expressed in HEK293 cells. Wbs are shown of total cell lysates of cells grown in starvation medium using the antibodies indicated to the right of each panel. Cortactin was immunoprecipitated, and immunoprecipitates were subjected to anti-pTyr Wb.

Deregulated Src-A activity is independent of Csk and can be rescued by an alternative PDZ ligand. Negative regulation of Src family kinases involves phosphorylation of Tyr527 (pY527) by Csk (8). Conserved residues in the kinase domain of Src family kinases specify the recognition of Src family kinases as substrates by Csk. All these residues are located N-terminal of Tyr527, indicating that the C-terminal GENL sequence is not required for Csk phosphorylation of c-Src (32, 50). However, to exclude the possibility that Src-A cannot be phosphorylated by Csk and hence displayed increased activity, we compared phosphorylation on Tyr527 of Src-L and Src-A. We expressed Src-L and Src-A or the kinase domains of Src-L or Src-A (SrcCT-L and SrcCT-A, respectively) in vitro and used them as substrates for purified active Csk (Fig. 2A). Phosphorylation of Tyr527 in Src was detected using anti-pY527 Src antibody. The addition of active Csk led to a substantial increase in pTyr527 in all Src proteins tested compared to the reactions carried out in the absence of Csk, and we detected no differences between Src-L and Src-A. To determine whether Src-A is an equally good substrate for Csk in cells, we probed total cell lysates of Src-L and Src-A cells with anti-pY527 Src antibody. No differences in pTyr527 were detectable, whereas Src-A phosphorylation of Tyr416 was increased (Fig. 2B).

We next determined whether the deregulated Src activity promoted by mutating the PDZ ligand sequence GENL to GENA could be rescued by replacing GENA with an artificial PDZ ligand sequence. To this end, we replaced GENA at the c-Src C terminus with STEV, a high-affinity binder for AF6 (44). Expression of Src-GENA in HEK293 cells increased the phosphorylation of Y416 Src, of total Tyr, and of cortactin (Fig. 2C). Expression of Src-STEV led to kinase activity and phosphorylation patterns comparable to those of cells expressing Src-GENL. Conversely, expression of Src-STEA, a mutation that does not bind AF6, displayed kinase activity and phosphorylation patterns similar to those of Src-GENA and reminiscent of deregulated Src activity. We detected no differences in Y527 Src phosphorylation between Src with an intact PDZ ligand sequence and Src with a mutated PDZ ligand sequence. Taken together, these data show that the Src activity and function toward endogenous substrates can be regulated by modifying the specificity of the Src C terminus for PDZ proteins by a mechanism that is independent of Csk phosphorylation of Src.

Src-A expression disrupts the morphology of acinar cultures. Overexpression of Src-A in mouse fibroblasts that do not express Src family kinases Src, Yes, and Fyn ($SYF^{-/-}$ cells)

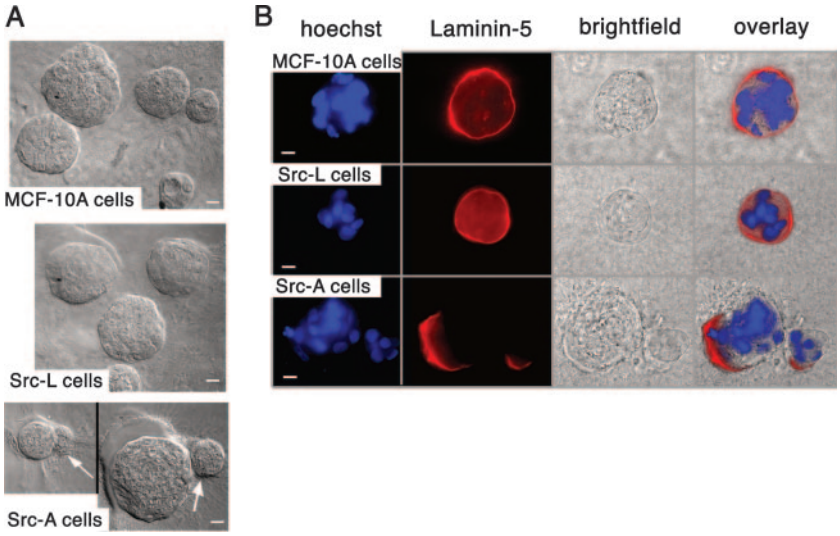

FIG. 3. Src-A expression in MCF-10A cells disrupts acinar cultures. (A) Bright-field images of 11-day acinar cultures of MCF-10A, Src-L, and Src-A cells. Arrows indicate clusters of cells that protrude from the original acinar culture. (B) IF microscopy images, as in panel A, with anti-Ln-5 antibody (red). Nuclei stained with Hoechst compound are in blue. Bars correspond to 20 μm.

promotes focus formation, anchorage-independent growth, and invasion (44). Therefore, we investigated whether Src-A interfered with morphogenetic processes or led to increased proliferation in nontransformed epithelial cells in three-dimensional cultures. MCF-10A cells seeded onto extracellular matrix grow into spheroids, named hereafter acinar cultures, and are characterized by a polarized alignment of cells and apoptosis of central cells that do not contact the BM (16).

Eleven-day acinar cultures derived from Src-A cells, but not from MCF-10A or Src-L cells, showed clusters of protruding cells (Fig. 3A, arrows). We stained the BM of acinar cultures with laminin-5 (Ln-5)-specific antibody and nuclei with Hoechst compound to determine the integrity of the BM by IF microscopy (Fig. 3B). The Ln-5 staining in all MCF-10A and Src-L acinar cultures enclosed all cells and appeared circular, whereas it was interrupted in some (approximately 25%) Src-A cultures and resembled a crescent moon with the opening toward the side of the protruding cell clusters. Neither in acinar nor in two-dimensional cultures did we observe increased proliferation of Src-A cells, suggesting that Src-A interfered with cell polarization rather than with cell proliferation to produce this phenotype.

Src-A impairs cell polarization during wound healing. To determine whether the C-terminal leucine in GENL is critical for cell polarization, we investigated collective cell migration after wounding, which requires cell polarization (17). Collective cell migration and wound healing in starved MCF-10A cells can be induced by EGF stimulation (34), and EGF-stimulated MCF-10A cells were able to close a 0.5-mm-wide scratch within 12 h (Fig. 4A; also see Movies S2 and S4 in the supplemental material). Migration was blocked in the presence of the Src kinase inhibitor PP2, implying that Src family kinase activity is required for efficient cell sheet migration (Fig. 4A; also see Movie S3 in the supplemental material). Src-L cells closed the wound within 12 h after EGF stimulation (Fig. 4B; also see Movie S5 in the supplemental material), whereas Src-A cells failed to close the wound within 12 h, with marginal cells displaying random rather than directed movements (Fig. 4B; also see Movie S6 in the supplemental material). Trajectories of migrating MCF-10A cells at the wound margin aligned parallel to an overall direction toward the wound (Fig. 4B). Trajectories of Src-L cells appeared more heterogeneous during the initial phase (at <4 h) but later aligned in a parallel direction (at >4 h). Src-A cells failed to align in parallel trajectories, with some cells even moving in opposing directions.

The failure of Src-A cells to establish directional persistence could result from impaired cell polarization toward the wound. In migrating, polarized cells, the Golgi apparatus is localized between the nucleus and the leading edge (6). We quantified Golgi apparatus orientation at 6 h after EGF-induced collective cell migration (Fig. 4C). Data revealed that 63% of the MCF-10A and 61% of the Src-L cells analyzed showed Golgi body localization between the leading edge and the nucleus. In contrast, Src-A expression led to a significant decrease of cell polarization because only 44% of Src-A cells displayed Golgi apparatus orientation toward the wound. Hence, the attenuated wound-directed migration of Src-A cells is in part the consequence of impaired polarization toward the wound.

To investigate whether the impaired polarization of Src-A cells could also contribute to the disruption of acinar cultures, we visualized Ln-5-positive BM and Golgi bodies in 11-day acinar cultures (Fig. 4D). Ln-5-positive BM delimited MCF-10A and Src-L acinar cultures. The Golgi apparatus of MCF-10A or Src-L cells localized on the side of the nucleus toward the center of the acinus, away from the BM, and indicated proper apicobasal polarization (49). In Src-A acinar cultures displaying a crescent moon-shaped Ln-5 staining pattern, cells escaped into the surrounding matrix with Golgi bodies oriented toward the presumable direction of migration. Taken together, Src-A expression impairs marginal cell polarization during EGF-induced collective cell sheet migration and apicobasal cell polarization in acinar cultures.

Src-A impairs localization of E-cadherin. The failure of Src-A cell polarization could be the result of a defect in cell-

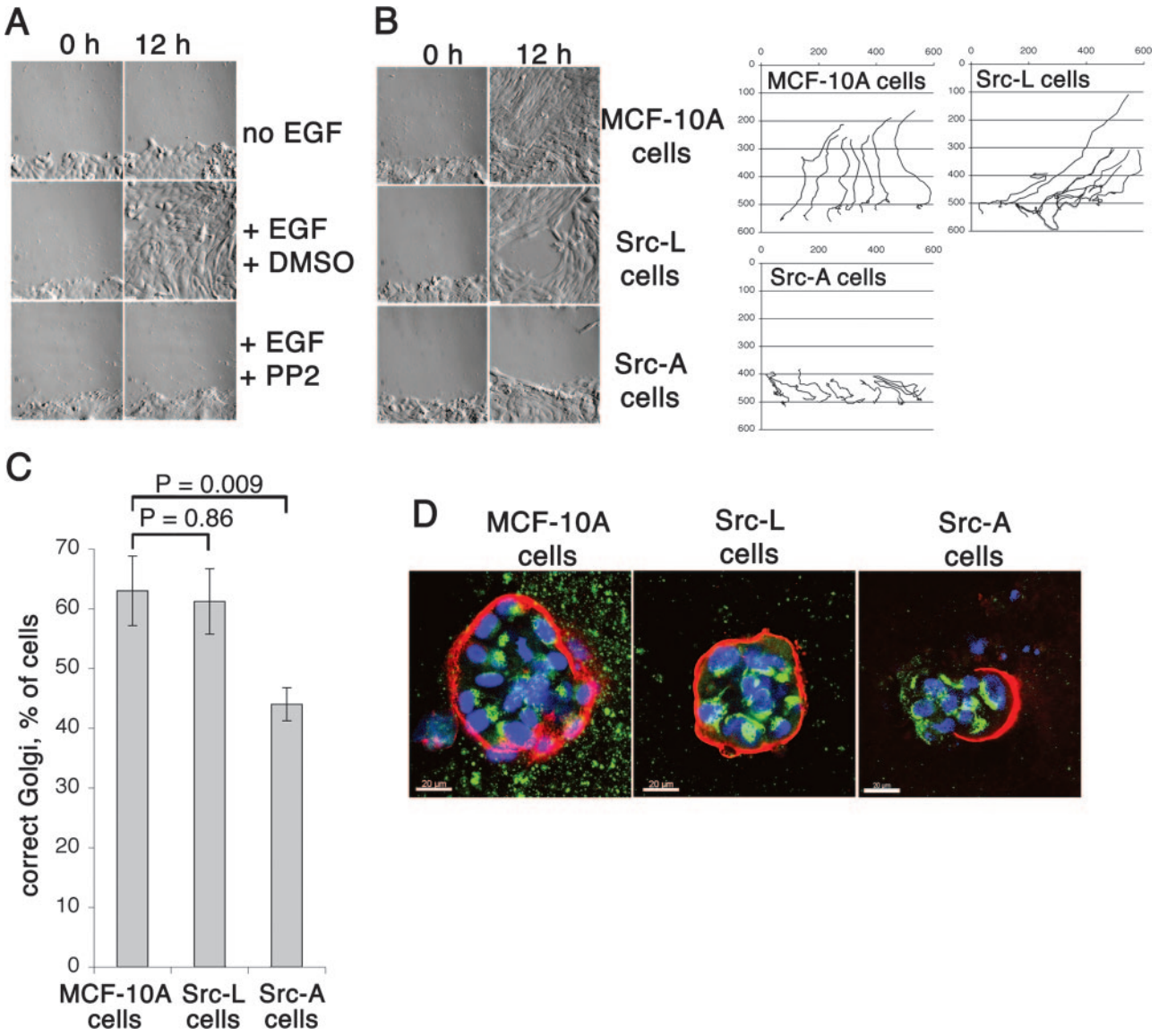

FIG. 4. Src-A expression impairs cell polarization. (A) Wound-healing assay. Where indicated, dimethyl sulfoxide (DMSO) solvent or 10 μM of Src kinase inhibitor PP2 was added. Wound healing was monitored for 12 h by live video microscopy. Still pictures are shown from video microscopy at 0 and 12 h (see Movies S1 to S3 in the supplemental material). (B) The same still images shown in panel A comparing the MCF-10A, Src-L, and Src-A cells (see Movies S4 to S6 in the supplemental material). Cells at the leading edge at 0 h were tracked for 12 h and plotted. Each line represents the path of one single cell over time. Axes are in digital pixels (0.64 μm/dp). (C) The Golgi apparatus was visualized by using anti-giantin antibody, and the position of the Golgi body relative to that of the nucleus was determined. Approximately 100 cells from five different fields were analyzed for each cell line, and the percentage of cells with correctly oriented Golgi bodies was determined. Bars show percentages of correctly oriented Golgi bodies and corresponding standard errors of the means. (D) Ln-5 (red), the Golgi apparatus (green), and the nuclei (blue) were visualized in 11-day acinar cultures by confocal IF microscopy. Bars correspond to 20 μm.

cell contact organization. Key players in epithelial cell-cell and cell-matrix adhesion are the adhesion molecule E-cadherin and its intracellular linker β-catenin (37). During wound healing, E-cadherin localized to regions of cell-cell contact up to the foremost rows of MCF-10A and Src-L cells (Fig. 5A, upper row). Src-A cells showed decreased and punctuated E-cadherin staining in regions of cell-cell contact. In complete growth medium, confluent monolayers of control cells displayed homogenous E-cadherin staining in regions of cell-cell contact, whereas the Src-A cell shape was irregular, and most cells displayed frayed E-cadherin staining (Fig. 5A, middle row). Analogous to that of E-cadherin, β-catenin was distributed in linear cell-cell contacts of MCF-10A and Src-L cells, whereas in Src-A cells, β-catenin was distributed along ridged, filamentous structures (Fig. 5A, lower row). These data suggest that GENL-regulated c-Src activity and localization (44) are required for the maintenance of cell sheet integrity and the proper E-cadherin and β-catenin localization in MCF-10A cells.

We next investigated E-cadherin localization with 11-day acinar cultures of MCF-10A, Src-L, and Src-A cells, using confocal IF microscopy. E-cadherin staining was detectable in

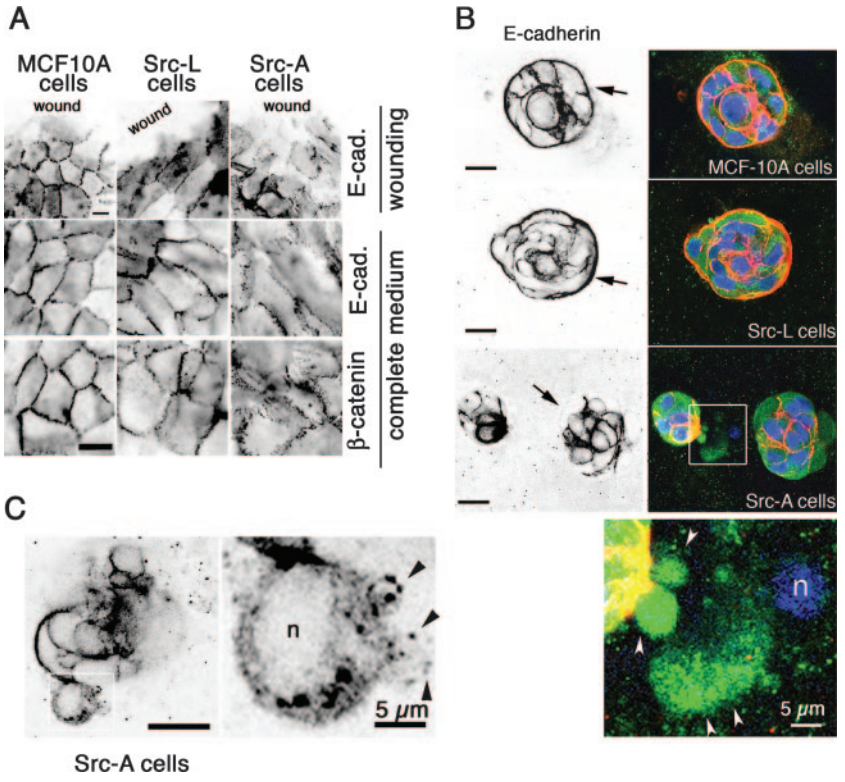

FIG. 5. Src-A expression impairs localization of E-cadherin. (A) Localization of E-cadherin during wound healing (8 h after wounding; top row) and in monolayers (middle row) or of β-catenin in monolayers (bottom row) was visualized by IF microscopy. For better visualization, IF staining is shown in the inverted mode. (B) Eleven-day acinar cultures of the MCF-10A, Src-L, and Src-A cells. Black and white images show inverted confocal IF of E-cadherin distribution. Color images show corresponding acinar cultures stained for E-cadherin (red), membrane protein palmitoylated 2 (green), and nuclei (blue). Arrows indicate the boundary between the acinar cultures and the ECM. Fourfold magnification of the framed area shows an escaping cell (arrowheads) with intact nucleus (n). (C) Confocal IF image of the Src-A acinar culture stained with anti-E-cadherin antibody. Arrowheads indicate punctuated E-cadherin staining in the escaping cell (fourfold magnification of the framed area). Bars correspond to 20 μm, unless otherwise stated.

regions of cell-cell contact (Fig. 5B). Interestingly, E-cadherin staining at the periphery of Src-A acinar cultures was decreased. Moreover, in Src-A acinar cultures, we found cells that protruded over the acinar margins (Fig. 5B). Cells protruding over the acinar margins displayed decreased E-cadherin staining (Fig. 5B) or E-cadherin staining in punctuated patterns (Fig. 5C, arrowheads), which might be indicative of increased E-cadherin endocytosis (5) induced by Src-A in peripheral regions in contact with BM proteins.

Src-A increases the velocity and directional persistence of cells migrating on BM. To determine whether Src-A cells respond differently to contact with the BM, we investigated adhesion to and single-cell migration on BM. Ln-5 is enriched in the BM of MCF-10A cells (38) and can be visualized with the Ln-5 γ2 chain-specific antibody (Fig. 8). Src-L or Src-A cells seeded onto prepared BM adhered and spread within 60 min (Fig. 6A), lamellipodia formed (Fig. 6A, arrowheads), and cells acquired a migratory phenotype. In the presence of the Src kinase inhibitor PP2, cells were still able to adhere to BM but no lamellipodia formed. We compared cell spreading by quantifying the area covered by individual Src-L and Src-A cells at 60 min after cells were seeded onto BM. We found that the average area covered by individual Src-A cells was twice the size of the area covered by Src-L cells (Fig. 6A, bar diagram). Inhibition of lamellipodium formation by PP2 indicated that Src kinase activity was necessary and implied Src kinase activation during adhesion. We tested this possibility by seeding Src-L and Src-A cells onto standard tissue culture plastic and determined the phosphorylation of Y416 Src (Fig. 6B). Src-L pY416 increased slightly within the first 5 min before returning to basal levels between 30 and 60 min later. Src-A pY416 increased similarly; however, the decline was less marked. To determine whether the BM might provide additional clues to Src activation, we monitored the phosphorylation of Y416 of Src-L and Src-A in cells seeded onto the BM (Fig. 6C). Src-L pY416 declined after 120 min, whereas Src-A pY416 remained elevated. Thus, our data suggest a negative regulatory role of GENL for Src kinase activation after adhesion.

We next determined by live cell video microscopy whether Src-A expression altered the motility of single cells on the BM. We used either starvation medium or starvation medium supplemented with 20 ng/ml EGF. We tracked individual cells (Fig. 6D) and quantified their velocity and directionality (Fig. 6E). The average velocity of MCF-10A cells was 0.96 μm/min without EGF and increased to 1.42 μm/min with EGF. Src-L velocity was 1.2 μm/min without EGF and 1.64 μm/min with EGF. Src-A velocity was 1.45 μm/min without EGF and 1.95

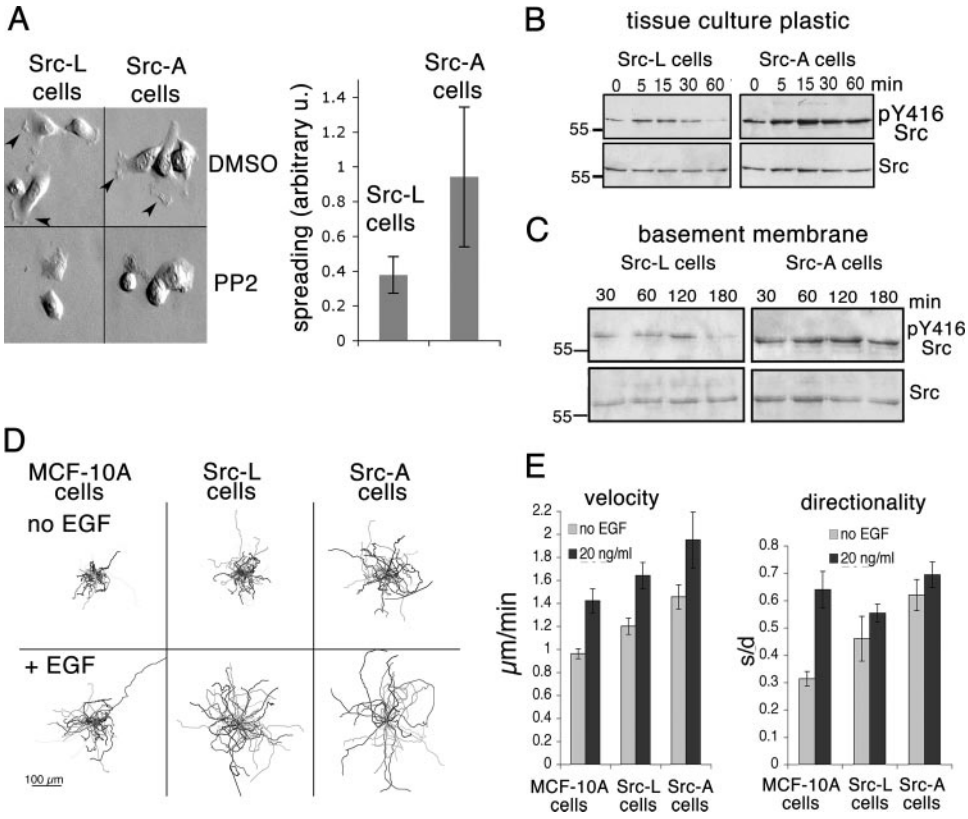

FIG. 6. Src-A increases velocity and directional persistence of migration on BM. (A) Src-L or Src-A cells seeded onto BM of MCF-10A cells in the presence of dimethyl sulfoxide (DMSO) solvent or of 10 μM PP2. Images were recorded 1 h after seeding. Arrowheads indicate lamellipodia in solvent-treated cells. The area covered by individual cells was quantified using NIH image software. Bars show averages of areas covered and standard deviations ($n = 19$ cells from four randomly selected spots). (B and C) Src-L and Src-A cells were trypsinized and kept in suspension in starvation medium for 1 h at 37°C, seeded onto regular tissue culture plastic (B) or onto the BM of MCF-10A cells (C), and lysed at the indicated time points after seeding. Wb of total cell lysates, using anti-Src2 and anti-pY416 Src antibodies. (D) MCF-10A, Src-L, or Src-A cells were seeded as described in the legend to panel C. Cells were left unstimulated or treated with EGF. Cell movements were recorded by live cell video microscopy over 2 h, tracked, and plotted. (E) The average velocity and median directionality of cells treated as described in the legend to panel D were determined. Average velocities ± standard errors of the means (SEM) were as follows: MCF-10A cells, 0.96 ± 0.043 μm/min without EGF and 1.42 ± 0.1 with EGF; Src-L cells, 1.2 ± 0.10 μm/min without EGF and 1.64 ± 0.11 μm/min with EGF; Src-A cells, 1.45 ± 0.1 μm/min without EGF and 1.95 ± 0.24 μm/min with EGF. Medians ± SEM of directionality were as follows: MCF-10A cells, 0.31 ± 0.026 without EGF and 0.64 ± 0.067 with EGF; Src-L cells, 0.46 ± 0.081 without EGF and 0.55 ± 0.033 with EGF; Src-A cells, 0.67 ± 0.057 without EGF and 0.69 ± 0.046 with EGF ($n = 45$ randomly selected cells from four experiments; *y*-axis error bars are SEM).

μm/min with EGF. The median directionality of MCF-10A cells was 0.31 without EGF and increased to 0.64 with EGF. Src-L cell directionality was 0.46 without EGF and 0.55 with EGF. Src-A cell directionality was 0.67 without EGF and 0.69 with EGF. These data show that Src-A expression increased velocity and directionality of single cells migrating on the BM in the absence of EGF stimulation to levels similar to that of EGF-stimulated control cells. In contrast, confluent Src-A cells failed to migrate directionally in monolayers during wound healing in the absence and presence of EGF (Fig. 4). The combination of cell sheet and single-cell migration analyses indicated that the C-terminal GENL sequence plays a regulatory role by modulating Src kinase activity and function downstream of cell-cell and cell-matrix adhesion. Hence, we suggest that intact c-Src is required to correctly integrate signals stemming from adhesion receptors into pathways regulating MCF-10A cell migration and that GENL is critically implicated in this process.

Src-A promotes phosphorylation of cortactin and FAK and their accumulation near the leading edge. The c-Src substrates cortactin and FAK are key regulators of cell migration (11). We therefore tested whether Src-A increased cortactin and FAK phosphorylation in motile cells on the c-Src-specific sites Y421 and Y861, respectively. We scratched multiple wounds into a subconfluent layer of cells to induce cell motility and compared the activation status of c-Src, Src-L, and Src-A and of cortactin and FAK after 12 h without and with EGF stimulation (Fig. 7A). The overall activities of c-Src, Src-L, and Src-A investigated by pY416 Src detection in scratched cells at low density (Fig. 7A) did not differ markedly from that of nonscratched cells grown at high density (Fig. 1D), and Y861 FAK phosphorylation levels were similar (Fig. 7A). In contrast, phospho-Y421 cortactin was detectable in scratched Src-A cells grown at low density (Fig. 7A) but not in nonscratched cells grown at high density (Fig. 1D). One possible explanation is that Src-A promotes translocation of cortactin

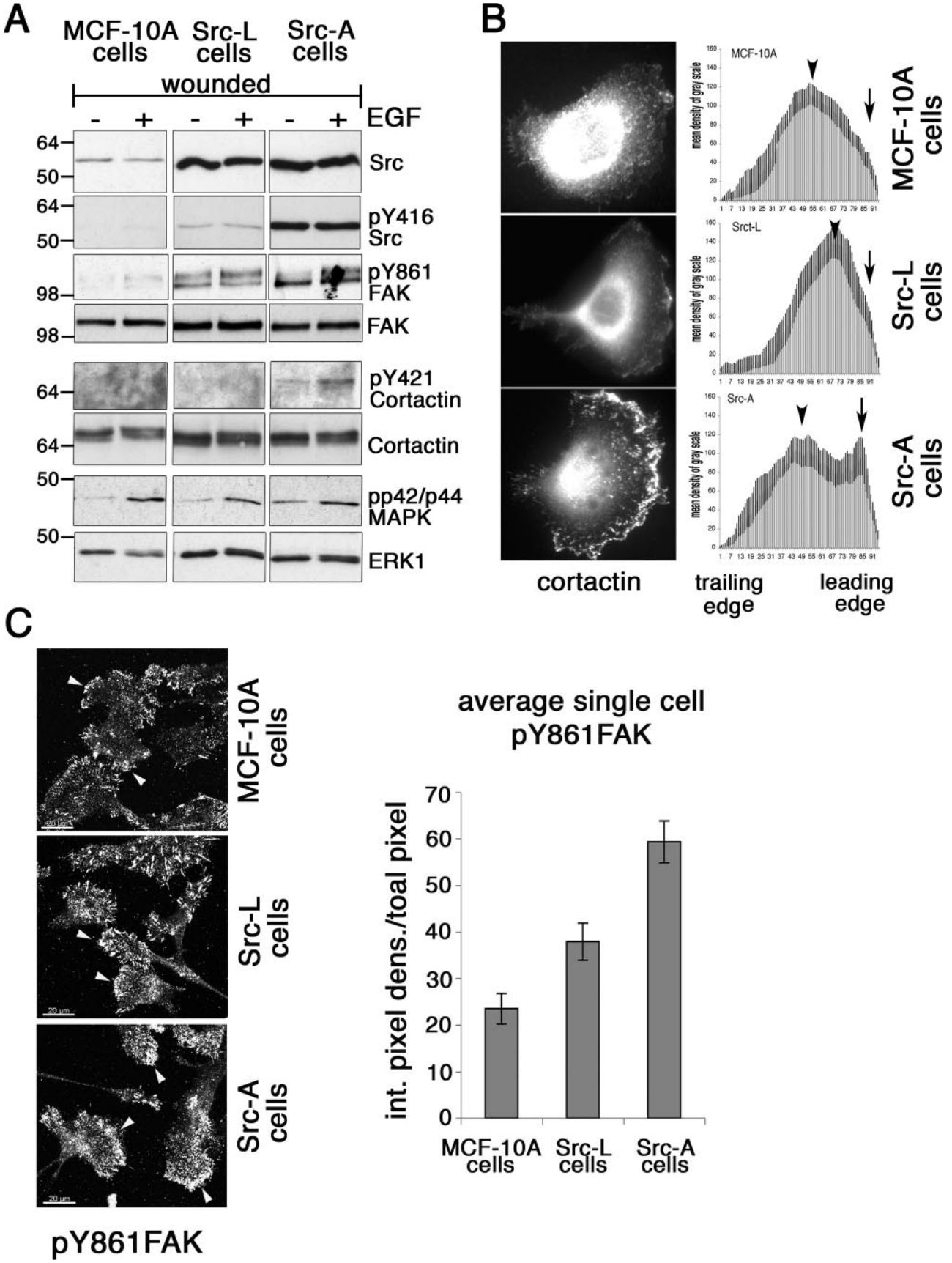
A
MCF-10A cells
Src-L cells
Src-A cells
wounded
- + - + - +
EGF
64
50
Src
64
50
pY416 Src
98
pY861 FAK
98
FAK
64
pY421 Cortactin
64
Cortactin
50
pp42/p44 MAPK
50
ERK1
B
cortactin
MCF-10A
Srct-L
Src-A
mean density of gray scale
MCF-10A cells
Src-L cells
Src-A cells
trailing edge
leading edge
C
MCF-10A cells
Src-L cells
Src-A cells
pY861FAK
average single cell pY861FAK
int. pixel dens./toal pixel
70
60
50
40
30
20
10
0
MCF-10A cells
Src-L cells
Src-A cells

and makes it accessible for phosphorylation. We therefore investigated cortactin localization in motile cells. We seeded MCF-10A, Src-L, and Src-A cells in starvation medium onto BM and visualized cortactin after 2 h by using standard IF (Fig. 7B). We quantified the fluorescence intensity of cortactin staining from the back to the front in cells that displayed a clearly polarized phenotype. Cortactin accumulated toward the leading edge (Fig. 7B, arrows) of Src-A cells but to a much lesser extent in Src-L or MCF-10A cells (Fig. 7B, bar diagrams). Together, these data show that Src-A increased cortactin Y421 phosphorylation and promoted cortactin localization toward the leading edge, possibly contributing to the increased persistence of migration (11) that we observed (Fig. 6E). FAK is required for the spatial organization of the leading edge of migrating cells (48), and FAK is a Src substrate in MCF-10A cells (Fig. 1 and 7). We therefore investigated whether Src-A increased pY861 FAK toward the leading edge, using confocal IF microscopy. As for the cortactin localization shown in Fig. 7B, we seeded cells in starvation medium onto BM for 2 h. Phospho-Y861 FAK was detectable in migrating MCF-10A, Src-L, and Src-A cells primarily at the basal side of lamellipodia and to a lesser extent in the cell body (Fig. 7C, arrowheads). Compared to MCF-10A cells, total pY861 FAK increased in Src-L cells and more markedly in Src-A cells (Fig. 7C, bar diagram). Hence, analogous to cortactin, the increased pY861 FAK shown in Fig. 7A is likely occurring in the lamella toward the leading edge.

A proteolytic activity that correlated with asymmetrically decreased Ln-5 in Src-A acinar cultures. Efficient migration of MCF-10A cells on BM correlated with FAK and cortactin recruitment to lamellipodia (Fig. 7) and requires cleavage of the Ln-5 γ chain by MT1-MMP (20). Src and FAK synergize to increase surface expression of MT1-MMP (54), cortactin and MT1-MMP interact at invadopodia (2), and MT1-MMP controls tumor cell traffic through the extracellular matrix (45). This suggested that Src-A might act through MT1-MMP to decrease Ln-5 staining in the BM surrounding acinar cultures (Fig. 3B) and to promote motility on BM (Fig. 6). We detected MT1-MMP on the lamellipodia of nonpermeabilized Src-L and Src-A cells (Fig. 8A, magnified areas) and in membrane fractions of MCF-10A, Src-L, or Src-A cells (Fig. 8F). To determine whether MT1-MMP localization correlated with proteolytic activity, we stained nonpermeabilized Src-L and Src-A cells seeded on BM with anti-Ln-5 antibody (Fig. 8B). Irregularly shaped black clouds were the result of low anti-Ln-5 staining in the intensively stained BM, which we considered a consequence of proteolytic activity. Overlaying the inverted Ln-5 fluorescence-stained image onto the bright-field image revealed that proteolytic activity concentrated underneath the lamellipodia (Fig. 8B, red coloring). MT1-MMP can process the Ln-5 p155 γ2 chain to the p105 γ2 chain by cleavage in domain III (Fig. 8C) (23). To quantify the Ln-5 γ2 chain processing in and around cells, we probed total cell lysates with anti-Ln-5 antibody, which is specific for domain III of the Ln-5 γ2 chain. We detected the native p155 γ2 chain containing domains I to V and the single processed p105 fragment (domains I to III) (Fig. 8D). To determine whether MT1-MMP activity toward the γ2 chain is altered by Src-A, we quantified the ratio between the p105 and the p155 γ2 chain (Fig. 8D, bar diagram). Src-A expression increased the level of Ln-5 γ2 chain expression and markedly increased the p105/p155 γ2 ratio.

MT1-MMP cleaves MMP2 and increases its activity in cell supernatants (28). We therefore investigated soluble (Fig. 8E) and membrane-bound (Fig. 8F) collagenase activities by gelatin zymography. Two main proteolytic activities were detectable in supernatants, which we assumed, based on their molecular weights, were MMP2 and MMP9 (Fig. 8E, arrows). Src-L and to a greater extent Src-A increased the overall proteolytic activity and the cleavage of MMP2 and MMP9 (Fig. 8E, arrowheads) in complete medium. In starved cells, we detected increased cleavage of MMP2 and MMP9 only in supernatants of Src-A cells. In membrane fractions, a protease activity of high molecular weight was markedly increased in Src-A cells (Fig. 8F, p170 in nondenaturing gel). We next investigated Ln-5 distribution and MT1-MMP expression in 11-day acinar cultures (Fig. 8G). MT1-MMP distributed to regions near the Ln-5-positive BM at the periphery of Src-L and Src-A acinar cultures. In the Src-A cells escaping from the acinar culture, MT1-MMP was also detectable at the leading edge (Fig. 8G, white arrow).

Taken together, we observed an increased proteolytic activity in Src-A cells toward the γ2 chain of Ln-5, a substrate for MT1-MMP. Proteolytic activity is increased underneath lamellipodia and correlates with the localization of MT1-MMP in single cells migrating on the BM and in Src-A acinar cultures.

DISCUSSION

We describe a novel mechanism for the maintenance of human breast epithelial cell sheet integrity and the prevention of an invasive phenotype induced by c-Src. This mechanism involves the c-Src C-terminal PDZ ligand sequence GENL (44). The GENL sequence is found in Src family kinase expressed in adherent cells but not in Hck, Lck, or Lyn, which are expressed in nonadherent cells, and suggests an important

FIG. 7. Src-A promotes phosphorylation of cortactin and FAK and leads to their accumulation toward the leading edge. (A) Wounds (160) were scratched into 50% confluent monolayers of starved MCF-10A, Src-L, and Src-A cells. Cells were then incubated without (−) or with (+) EGF for 12 h. Wb of total cell lysates, using the antibodies indicated, is shown. (B) MCF-10A, Src-L, or Src-A cells were seeded in starvation medium onto BM. Two hours after cells were seeded, cortactin was visualized by IF microscopy. Average fluorescence intensities of one-pixel-wide sections across clearly polarized cells ($n = 6$ polarized cells per cell line) were determined by using NIH image software and plotted. The orientation is trailing-to-leading edge; the dark gray bars are standard error of the mean (SEM) densities of grayscale fluorescence. Arrows indicate approximate positions of peak fluorescence near leading edges; arrowheads indicate the centers of gravity (peak fluorescence near the nucleus). (C) The MCF-10A, Src-L, and Src-A cells were seeded onto the BM as described in the legend to panel B. Phosphorylation of Y861 FAK was determined by confocal IF microscopy. Arrowheads indicate Y861 FAK phosphorylation at leading edges. The bar diagram shows the averages of integrated pixel densities per cell of 15 cells. Error bars are SEM.

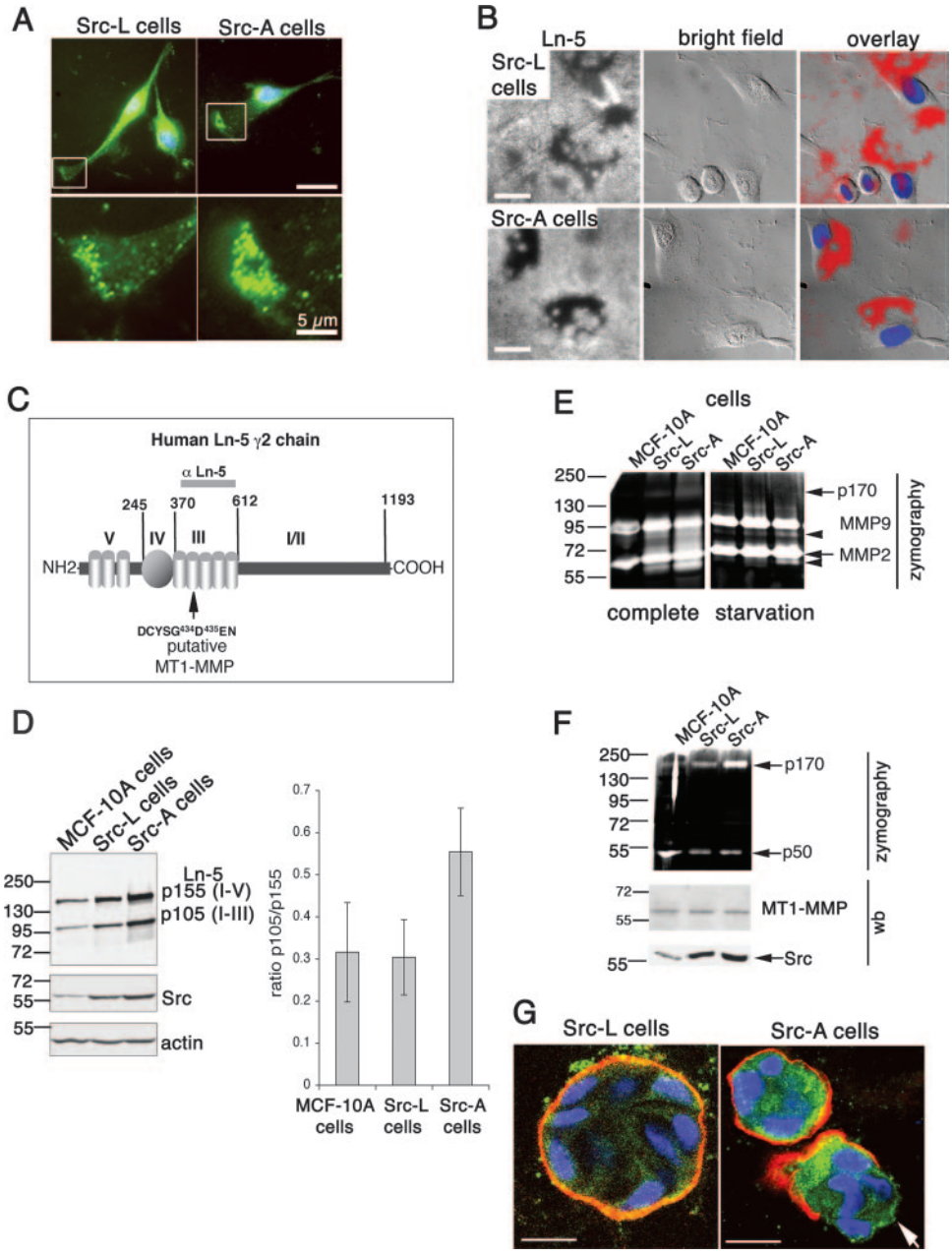

FIG. 8. Increased Ln-5 processing in Src-A cells. (A) MT1-MMP (green) and nuclei (blue) were visualized by IF microscopy of nonpermeabilized Src-L or Src-A cells at 3 h after cells were seeded onto BM in starvation medium. (B) The MCF-10A, Src-L, and Src-A cells were seeded, and Ln-5 was visualized as described in the legend to panel A (Ln-5). Grayscale Ln-5 fluorescence was inverted and overlaid onto bright-field images (overlay). Areas with decreased Ln-5 are in red. (C) Schema of human Ln-5 γ2 chain with the putative MT1-MMP cleavage site within laminin-type EGF-like subdomains of domain III (according to rat Ln-5 γ2 chain [46]). (D) Wbs of the Ln-5 γ2 p155 and p105 chains in total MCF-10A, Src-L, and Src-A cell extracts using anti-Ln-5 antibody. Expression controls for Src and actin are shown. Pixel densities of the p155 and p105 bands from three independent experiments were quantified, and the ratio of p105/p155 was determined (error bars are standard errors of the means). (E) Gelatin zymography using supernatants of the MCF-10A, Src-L, and Src-A cells grown for 18 h in complete or starvation medium. (F) Gelatin zymography and Wb using membrane extracts of the MCF-10A, Src-L, and Src-A cells grown for 18 h in complete medium. SDS-PAGE was performed under nondenaturing conditions. (G) Ln-5 (red), MT1-MMP (green), and nuclei (blue) were visualized in 11-day acinar cultures by IF confocal microscopy. Bars correspond to 20 μm, unless otherwise stated.

function of GENL in c-Src regulation in adherent cells. Our investigation of the biological relevance of C-terminal leucine in GENL in regulating c-Src strongly supports a model where GENL is a regulatory sequence specific for Src family kinases of adherent cells (Fig. 9). We ascribe the regulatory function of the intact GENL sequence to maintaining c-Src in a resting state in starved cells and to limiting the phosphorylation of specific substrates after stimulation by growth factor or adhesion receptors. Our data indicate that the pleiotropic effects of a C-terminal Leu/Ala mutation are the consequence of the

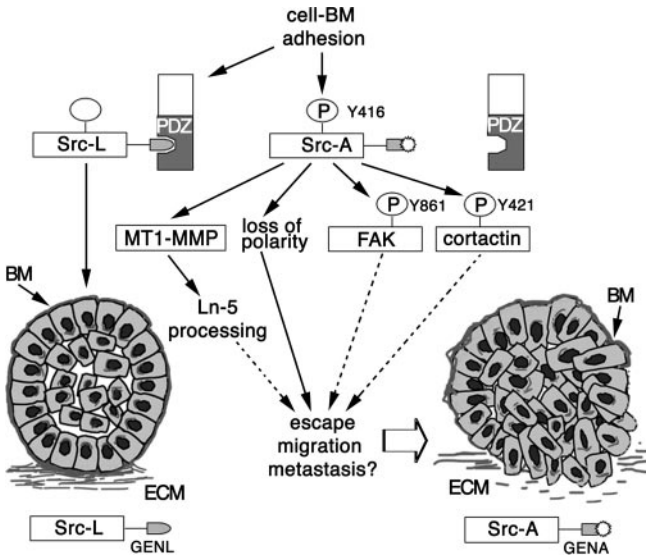

FIG. 9. Model of the c-Src GENL sequence regulation of the invasion-promoting potential of c-Src. Replacement of the C-terminal leucine in the c-Src GENL sequence with alanine increased Src activity in cells and its potential to promote adhesion-induced cell migration by increasing the localized activation of cortactin and FAK and by promoting pericellular proteolysis. A combination thereof may lead to the establishment of impaired polarity during wound healing and, in acinar cultures, to the escape of cells into the surrounding ECM.

capability of intact GENL to restrict multiple c-Src functions in human breast epithelial cells, such as substrate activation, cell-cell contact disassembly, induction of haptotactic cell motility, and promotion of basement membrane degradation. Our data also highlight elements of c-Src function in epithelial cell homeostasis and progression toward an invasive phenotype that previously have been addressed only with "oncogenically" activated or viral Src kinases.

The kinase activity of Src-A in vitro is similar to that of Src-L (44). Hence, it was proposed that the interaction of c-Src with PDZ proteins occurs or is strengthened by means of the GENL sequence and leads to a spatial and functional restriction of c-Src activity in cells. We found that negative regulation of c-Src activity by C-terminal Leu is more marked under conditions of starvation, suggesting that the interaction with a PDZ protein occurs particularly in the absence of growth factors. We observed that Src-A expression in acinar cultures does not induce hyperproliferation. It is thus unlikely that Src-A mediates proliferation-promoting signaling from receptor tyrosine kinase. Instead, we concluded that GENL restricts c-Src activity downstream of adhesion to the BM for several reasons. Src-A Y416 phosphorylation is increased compared to that of Src-L in adherent, unstimulated cells. Unlike that of Src-L, however, Src-A Y416 phosphorylation is not increased further by growth factor stimulation. Furthermore, adhesion to BM increased Src-A Y416 phosphorylation and prolonged it compared to that of Src-L. Moreover, Src-A increased the spreading of MCF-10A cells on BM. The presence of Src-A promoted growth factor-independent motility of MCF-10A cells on BM, and Src-A increased phosphorylation and translocation of specific substrates during migration on BM. Finally, EGF stimulation of Src-A cells was not sufficient to overcome adhesion signals in wound healing.

Src-A promotes adhesion-induced MCF-10A single-cell migration, indicating that GENL may restrict signaling of c-Src after contact with the BM. Impairing this function prolongs Src activation after adhesion to BM and promotes a migratory behavior in Src-A cells similar to that of the EGF-stimulated control cells. Analogously, faulty "sensing" of the BM in Src-A acinar cultures may lead to polarization defects and the escape of Src-A-expressing cells into the surrounding extracellular matrix (ECM). Polarity defects in Src-A acinar cultures resemble polarity defects in the malignant breast tumor cell line HMT-3522 (33), where a constitutively active phosphatidylinositol 3-kinase deregulates polarity through the small GTPase Rac. Rac is activated by c-Src downstream of E-cadherin (19), suggesting that impaired polarity could be the result of Src-A activating the Rac pathway. Increased Src-A activation could be the result of constitutive Src-A-integrin interaction, followed by deregulated activation when integrins engage with the ECM (1, 10). Alternatively, FAK phosphorylated at Y397 could lead to increased Src-A recruitment to and activation in focal adhesions (55). Consistently, we observed increased FAK phosphorylation on the Src-specific Y861 in Src-A cells. This raises the possibility that c-Src GENL in MCF-10A cells coordinates the synergy between c-Src and FAK, which is required for effective focal adhesion turnover at the cell front (51) and the spatial organization of the leading edge of migrating fibroblasts (48).

Cortactin, another Src substrate (25, 53), is involved in regulating the leading edge of migrating cells by controlling actin polymerization (31) and lamellipodial dynamics (11). Src phosphorylation of cortactin negatively regulates cortactin functions (25, 36). However, tyrosine phosphorylation of cortactin may increase F-actin turnover to promote actin dynamics in migrating cells (14), which would now be supported by our data showing increased cortactin Y421 phosphorylation and recruitment to the leading edge in cells that migrate efficiently.

Cortactin organizes invadopodia at the ventral side of invasive breast cancer cells structurally to form membrane protrusions and functionally to deliver MT1-MMP (2). c-Src expression increases invasion mediated by invadopodia (2) and promotes the colocalization of cortactin with tyrosine-phosphorylated proteins at invadopodia (9). Hence, modulation of cortactin phosphorylation and localization by Src-A indicate that GENL may restrict invadopodium formation and decrease pericellular proteolytic activity induced by activated c-Src. This possibility is strengthened by our findings that Src-A increases the release of cleaved MMP2 into the supernatant and promotes Ln-5 γ2 chain cleavage and degradation of the BM. In Src-A single cells on the BM, increased pericellular proteolytic activity could promote cell migration by modifying the substratum (20, 30) or by the production of EGF-like Ln-5 fragments that stimulate the EGF receptor (46).

Which are the PDZ proteins that likely regulate c-Src functions in the epithelial cells that we described herein is unclear. One candidate, AF6, is a multidomain protein containing one PDZ domain and was found to regulate c-Src function in epithelial cells (44). AF6 promotes the formation of cell-cell contacts by increasing E-cadherin-p120 interaction and by coordinating E-cadherin-actin interaction (34). Both the AF6

knockdown MCF-10A cells and the Src-A cells display decreased cell-cell contacts in wound healing experiments, and similarly to Src-A cells, AF6 knockdown cells do display increased pY861 FAK (34, 44). Moreover, we found that the PDZ ligand sequence STEV, a high-affinity ligand for AF6, rescues the restriction of Src in cells. However, the overall phenotype of AF6 knockdown in MCF-10A cells is not entirely copied in Src-A cells, because AF6 knockdown MCF-10A cells migrating on the BM display velocity equal to that of control cells (M. Baumgartner, unpublished). Hence, this partial parallel behavior of the AF6 knockdown cells and the Src-A cells indicates that AF6 is involved in c-Src regulation and that additional PDZ proteins are likely involved in MCF-10A cells.

More than 10% of all human protein kinases contain a putative PDZ ligand sequence at their C terminus. Therefore, the regulation of protein kinases through PDZ domain interaction may be a common mechanism of kinase regulation. The identification of further c-Src-regulating PDZ domain proteins will be an important future task as it may also provide novel avenues for therapeutic interventions in pathologies implicating c-Src kinase activation, such as cancer cell metastasis.

ACKNOWLEDGMENTS

We thank Matthias Hoechli and the electron- and light microscopy facility (EMZ) for excellent support for live cell imaging and confocal microscopy.

This work was supported in part by the Swiss National Science Foundation (K. Moelling).

REFERENCES

1. **Arias-Salgado, E. G., S. Lizano, S. Sarkar, J. S. Brugge, M. H. Ginsberg, and S. J. Shattil.** 2003. Src kinase activation by direct interaction with the integrin beta cytoplasmic domain. Proc. Natl. Acad. Sci. USA **100:**13298–13302.
2. **Artym, V. V., Y. Zhang, F. Seillier-Moiseiwitsch, K. M. Yamada, and S. C. Mueller.** 2006. Dynamic interactions of cortactin and membrane type 1 matrix metalloproteinase at invadopodia: defining the stages of invadopodia formation and function. Cancer Res. **66:**3034–3043.
3. **Avizienyte, E., V. G. Brunton, V. J. Fincham, and M. C. Frame.** 2005. The SRC-induced mesenchymal state in late-stage colon cancer cells. Cells Tissues Organs **179:**73–80.
4. **Avizienyte, E., V. J. Fincham, V. G. Brunton, and M. C. Frame.** 2004. Src SH3/2 domain-mediated peripheral accumulation of Src and phospho-myosin is linked to deregulation of E-cadherin and the epithelial-mesenchymal transition. Mol. Biol. Cell **15:**2794–2803.
5. **Avizienyte, E., and M. C. Frame.** 2005. Src and FAK signalling controls adhesion fate and the epithelial-to-mesenchymal transition. Curr. Opin. Cell Biol. **17:**542–547.
6. **Bershadsky, A. D., and A. H. Futerman.** 1994. Disruption of the Golgi apparatus by brefeldin A blocks cell polarization and inhibits directed cell migration. Proc. Natl. Acad. Sci. USA **91:**5686–5689.
7. **Biscardi, J. S., A. P. Belsches, and S. J. Parsons.** 1998. Characterization of human epidermal growth factor receptor and c-Src interactions in human breast tumor cells. Mol. Carcinog. **21:**261–272.
8. **Boggon, T. J., and M. J. Eck.** 2004. Structure and regulation of Src family kinases. Oncogene **23:**7918–7927.
9. **Bowden, E. T., E. Onikoyi, R. Slack, A. Myoui, T. Yoneda, K. M. Yamada, and S. C. Mueller.** 2006. Co-localization of cortactin and phosphotyrosine identifies active invadopodia in human breast cancer cells. Exp. Cell Res. **312:**1240–1253.
10. **Brunton, V. G., I. R. MacPherson, and M. C. Frame.** 2004. Cell adhesion receptors, tyrosine kinases and actin modulators: a complex three-way circuitry. Biochim. Biophys. Acta **1692:**121–144.
11. **Bryce, N. S., E. S. Clark, J. L. Leysath, J. D. Currie, D. J. Webb, and A. M. Weaver.** 2005. Cortactin promotes cell motility by enhancing lamellipodial persistence. Curr. Biol. **15:**1276–1285.
12. **Carragher, N. O., M. A. Westhoff, V. J. Fincham, M. D. Schaller, and M. C. Frame.** 2003. A novel role for FAK as a protease-targeting adaptor protein: regulation by p42 ERK and Src. Curr. Biol. **13:**1442–1450.
13. **Chiaradonna, F., L. Fontana, C. Iavarone, M. V. Carriero, G. Scholz, M. V. Barone, and M. P. Stoppelli.** 1999. Urokinase receptor-dependent and -independent p56/59(hck) activation state is a molecular switch between myelomonocytic cell motility and adherence. EMBO J. **18:**3013–3023.
14. **Cosen-Binker, L. I., and A. Kapus.** 2006. Cortactin: the gray eminence of the cytoskeleton. Physiology (Bethesda) **21:**352–361.
15. **Cowan-Jacob, S. W., G. Fendrich, P. W. Manley, W. Jahnke, D. Fabbro, J. Liebetanz, and T. Meyer.** 2005. The crystal structure of a c-Src complex in an active conformation suggests possible steps in c-Src activation. Structure **13:**861–871.
16. **Debnath, J., and J. S. Brugge.** 2005. Modelling glandular epithelial cancers in three-dimensional cultures. Nat Rev. Cancer **5:**675–688.
17. **Farooqui, R., and G. Fenteany.** 2005. Multiple rows of cells behind an epithelial wound edge extend cryptic lamellipodia to collectively drive cell-sheet movement. J. Cell Sci. **118:**51–63.
18. **Frame, M. C.** 2004. Newest findings on the oldest oncogene: how activated src does it. J. Cell Sci. **117:**989–998.
19. **Fukuyama, T., H. Ogita, T. Kawakatsu, M. Inagaki, and Y. Takai.** 2006. Activation of Rac by cadherin through the c-Src-Rap1-phosphatidylinositol 3-kinase-Vav2 pathway. Oncogene **25:**8–19.
20. **Gilles, C., M. Polette, C. Coraux, J. M. Tournier, G. Meneguzzi, C. Munaut, L. Volders, P. Rousselle, P. Birembaut, and J. M. Foidart.** 2001. Contribution of MT1-MMP and of human laminin-5 gamma2 chain degradation to mammary epithelial cell migration. J. Cell Sci. **114:**2967–2976.
21. **Gonzalez, L., M. T. Agullo-Ortuno, J. M. Garcia-Martinez, A. Calcabrini, C. Gamallo, J. Palacios, A. Aranda, and J. Martin-Perez.** 2006. Role of c-Src in human MCF7 breast cancer cell tumorigenesis. J. Biol. Chem. **281:**20851–20864.
22. **Heinrich, J., M. Bosse, H. Eickhoff, W. Nietfeld, R. Reinhardt, H. Lehrach, and K. Moelling.** 2000. Induction of putative tumor-suppressing genes in Rat-1 fibroblasts by oncogenic Raf-1 as evidenced by robot-assisted complex hybridization. J. Mol. Med. **78:**380–388.
23. **Hintermann, E., and V. Quaranta.** 2004. Epithelial cell motility on laminin-5: regulation by matrix assembly, proteolysis, integrins and erbB receptors. Matrix Biol. **23:**75–85.
24. **Hsia, D. A., S. K. Mitra, C. R. Hauck, D. N. Streblow, J. A. Nelson, D. Ilic, S. Huang, E. Li, G. R. Nemerow, J. Leng, K. S. Spencer, D. A. Cheresh, and D. D. Schlaepfer.** 2003. Differential regulation of cell motility and invasion by FAK. J. Cell Biol. **160:**753–767.
25. **Huang, C., Y. Ni, T. Wang, Y. Gao, C. C. Haudenschild, and X. Zhan.** 1997. Down-regulation of the filamentous actin cross-linking activity of cortactin by Src-mediated tyrosine phosphorylation. J. Biol. Chem. **272:**13911–13915.
26. **Ilic, D., Y. Furuta, S. Kanazawa, N. Takeda, K. Sobue, N. Nakatsuji, S. Nomura, J. Fujimoto, M. Okada, and T. Yamamoto.** 1995. Reduced cell motility and enhanced focal adhesion contact formation in cells from FAK-deficient mice. Nature **377:**539–544.
27. **Ishizawar, R., and S. J. Parsons.** 2004. c-Src and cooperating partners in human cancer. Cancer Cell **6:**209–214.
28. **Itoh, Y., and M. Seiki.** 2004. MT1-MMP: an enzyme with multidimensional regulation. Trends Biochem. Sci. **29:**285–289.
29. **Kim, E., S. J. DeMarco, S. M. Marfatia, A. H. Chishti, M. Sheng, and E. E. Strehler.** 1998. Plasma membrane Ca2+ ATPase isoform 4b binds to membrane-associated guanylate kinase (MAGUK) proteins via their PDZ (PSD-95/Dlg/ZO-1) domains. J. Biol. Chem. **273:**1591–1595.
30. **Koshikawa, N., S. Schenk, G. Moeckel, A. Sharabi, K. Miyazaki, H. Gardner, R. Zent, and V. Quaranta.** 2004. Proteolytic processing of laminin-5 by MT1-MMP in tissues and its effects on epithelial cell morphology. FASEB J. **18:**364–366.
31. **Kowalski, J. R., C. Egile, S. Gil, S. B. Snapper, R. Li, and S. M. Thomas.** 2005. Cortactin regulates cell migration through activation of N-WASP. J. Cell Sci. **118:**79–87.
32. **Lee, S., M. K. Ayrapetov, D. J. Kemble, K. Parang, and G. Sun.** 2006. Docking-based substrate recognition by the catalytic domain of a protein tyrosine kinase, C-terminal Src kinase (Csk). J. Biol. Chem. **281:**8183–8189.
33. **Liu, H., D. C. Radisky, F. Wang, and M. J. Bissell.** 2004. Polarity and proliferation are controlled by distinct signaling pathways downstream of PI3-kinase in breast epithelial tumor cells. J. Cell Biol. **164:**603–612.
34. **Lorger, M., and K. Moelling.** 2006. Regulation of epithelial wound closure and intercellular adhesion by interaction of AF6 with actin cytoskeleton. J. Cell Sci. **119:**3385–3398.
35. **Martin, G. S.** 2001. The hunting of the Src. Nat. Rev. Mol. Cell Biol. **2:**467–475.
36. **Martinez-Quiles, N., H.-Y. Ho, M. W. Kirschner, N. Ramesh, and R. S. Geha.** 2004. Erk/Src phosphorylation of cortactin acts as a switch on-switch off mechanism that controls its ability to activate N-WASP. Mol. Cell. Biol. **24:**5269–5280.
37. **Mege, R. M., J. Gavard, and M. Lambert.** 2006. Regulation of cell-cell junctions by the cytoskeleton. Curr. Opin. Cell Biol. **18:**541–548.
38. **Miller, K. A., J. Chung, D. Lo, J. C. Jones, B. Thimmapaya, and S. A. Weitzman.** 2000. Inhibition of laminin-5 production in breast epithelial cells by overexpression of p300. J. Biol. Chem. **275:**8176–8182.
39. **Mitra, S. K., and D. D. Schlaepfer.** 2006. Integrin-regulated FAK-Src signaling in normal and cancer cells. Curr. Opin. Cell Biol. **18:**516–523.
40. **Nelson, C. M., and M. J. Bissell.** 2005. Modeling dynamic reciprocity: engineering three-dimensional culture models of breast architecture, function, and neoplastic transformation. Semin. Cancer Biol. **15:**342–352.

41. **Nobes, C. D., and A. Hall.** 1999. Rho GTPases control polarity, protrusion, and adhesion during cell movement. J. Cell Biol. **144:**1235–1244.
42. **Nourry, C., S. G. Grant, and J. P. Borg.** 2003. PDZ domain proteins: plug and play! Sci. STKE **2003:**RE7.
43. **O'Brien, L. E., M. M. Zegers, and K. E. Mostov.** 2002. Opinion: building epithelial architecture: insights from three-dimensional culture models. Nat. Rev. Mol. Cell Biol. **3:**531–537.
44. **Radziwill, G., A. Weiss, J. Heinrich, M. Baumgartner, P. Boisguerin, K. Owada, and K. Moelling.** 2007. Regulation of c-Src by binding to the PDZ domain of AF-6. EMBO J. **26:**2633–2644.
45. **Sabeh, F., I. Ota, K. Holmbeck, H. Birkedal-Hansen, P. Soloway, M. Balbin, C. Lopez-Otin, S. Shapiro, M. Inada, S. Krane, E. Allen, D. Chung, and S. J. Weiss.** 2004. Tumor cell traffic through the extracellular matrix is controlled by the membrane-anchored collagenase MT1-MMP. J. Cell Biol. **167:**769–781.
46. **Schenk, S., E. Hintermann, M. Bilban, N. Koshikawa, C. Hojilla, R. Khokha, and V. Quaranta.** 2003. Binding to EGF receptor of a laminin-5 EGF-like fragment liberated during MMP-dependent mammary gland involution. J. Cell Biol. **161:**197–209.
47. **Schlaepfer, D. D., S. K. Mitra, and D. Ilic.** 2004. Control of motile and invasive cell phenotypes by focal adhesion kinase. Biochim. Biophys. Acta **1692:**77–102.
48. **Tilghman, R. W., J. K. Slack-Davis, N. Sergina, K. H. Martin, M. Iwanicki, E. D. Hershey, H. E. Beggs, L. F. Reichardt, and J. T. Parsons.** 2005. Focal adhesion kinase is required for the spatial organization of the leading edge in migrating cells. J. Cell Sci. **118:**2613–2623.
49. **Underwood, J. M., K. M. Imbalzano, V. M. Weaver, A. H. Fischer, A. N. Imbalzano, and J. A. Nickerson.** 2006. The ultrastructure of MCF-10A acini. J. Cell. Physiol. **208:**141–148.
50. **Wang, D., X. Y. Huang, and P. A. Cole.** 2001. Molecular determinants for Csk-catalyzed tyrosine phosphorylation of the Src tail. Biochemistry **40:** 2004–2010.
51. **Webb, D. J., K. Donais, L. A. Whitmore, S. M. Thomas, C. E. Turner, J. T. Parsons, and A. F. Horwitz.** 2004. FAK-Src signalling through paxillin, ERK and MLCK regulates adhesion disassembly. Nat. Cell Biol. **6:**154–161.
52. **Wrobel, C. N., J. Debnath, E. Lin, S. Beausoleil, M. F. Roussel, and J. S. Brugge.** 2004. Autocrine CSF-1R activation promotes Src-dependent disruption of mammary epithelial architecture. J. Cell Biol. **165:**263–273.
53. **Wu, H., and J. T. Parsons.** 1993. Cortactin, an 80/85-kilodalton pp60src substrate, is a filamentous actin-binding protein enriched in the cell cortex. J. Cell Biol. **120:**1417–1426.
54. **Wu, X., B. Gan, Y. Yoo, and J. L. Guan.** 2005. FAK-mediated src phosphorylation of endophilin A2 inhibits endocytosis of MT1-MMP and promotes ECM degradation. Dev. Cell **9:**185–196.
55. **Yeo, M. G., M. A. Partridge, E. J. Ezratty, Q. Shen, G. G. Gundersen, and E. E. Marcantonio.** 2006. Src SH2 arginine 175 is required for cell motility: specific focal adhesion kinase targeting and focal adhesion assembly function. Mol. Cell. Biol. **26:**4399–4409.